

# The thermal decomposition of 5-membered rings: a laser pyrolysis study

Nathan R. Hore and Douglas K. Russell\*

Department of Chemistry, University of Auckland, Private Bag 92019, Auckland, New Zealand.  
E-mail: d.russell@auckland.ac.nz; Fax: +64 9 373 7422

Received (in Montpellier, France) 20th November 2003, Accepted 19th January 2004  
First published as an Advance Article on the web 1st April 2004

The mechanisms of pyrolysis of cyclopentadiene, furan, pyrrole and thiophene have been investigated using a combination of IR laser powered homogeneous pyrolysis, chemical and physical trapping of radical intermediates, and use of precursors specifically designed to generate selected radical intermediates. The results confirm the central role played by free radicals in the cases of cyclopentadiene and thiophene, and the dominant step of 1,2-H shifts in the cases of furan and pyrrole. The experimental results may be interpreted according to the high level *ab initio* calculations recently reported in the literature.

## Introduction

The mechanism of pyrolysis of 5-membered cyclic compounds is of considerable interest in our understanding of combustion. In particular, systems such as furan, pyrrole, cyclopentadiene and especially thiophene have all been implicated as significant species in the pyrolysis of fossil fuels.<sup>1</sup> In addition, furan has also been identified as a significant component of tobacco smoke,<sup>2</sup> while the pyrolysis of thiophene has applications in the synthesis of conducting polymers.<sup>3</sup> While there have been several experimental studies of the kinetics of decomposition of furan,<sup>1,4-6</sup> pyrrole<sup>1,7-11</sup> and cyclopentadiene<sup>1,12-17</sup> with some mechanistic interpretation, there has been rather little experimental work specifically directed towards full elucidation of mechanistic detail, and very little at all has been published on thiophene apart from a very recent product-oriented investigation.<sup>18</sup> On the other hand, a number of recent high-level theoretical investigations have thrown new light on possible reaction routes.<sup>19-24</sup>

We have shown that the technique of infrared laser powered homogeneous pyrolysis (IR LPHP), allied with standard mechanistic tools such as matrix isolation spectroscopies, reaction in the presence of trapping agents, and *ab initio* or semi-empirical calculation of activation energies, can provide unique insights into the mechanisms of pyrolysis in systems as varied as azines,<sup>25</sup> organometallic chemical vapour deposition (CVD) precursors,<sup>26-31</sup> glycine<sup>32</sup> and chlorofluorocarbons.<sup>33</sup> In particular, the use of matrix isolation EPR spectroscopy and of radical traps such as H<sub>2</sub> or D<sub>2</sub> allows the disentanglement of molecular and radical pathways. In the case of azines,<sup>25</sup> we have also shown that the use of precursors specifically designed to proceed through relevant radical pathways, principally bromine-substituted analogues, allows even more detailed mechanistic information. In the present work, we apply these techniques to a study of the 5-membered ring systems cyclopentadiene, pyrrole, furan and thiophene.

## Experimental methods and calculations

### Compounds

All compounds used in this study, with the exception of 2-bromofuran, were 'AR' grade (Aldrich or Lancaster); these and SF<sub>6</sub> (BOC) were purified prior to use by repeated freeze-pump-thaw cycles. 2-Bromofuran was synthesised from

5-bromofuroic acid according to the method of Clennan and Mehrsheikh-Mohammabi,<sup>34</sup> and the purity of the final product checked using GC/MS. Since cyclopentadiene dimerises at room temperature, the vapour of the monomer was generated by heating the pyrolysis cell (see below) at a temperature insufficient to induce further pyrolysis; the exclusive presence of the monomer was verified by FTIR spectroscopy. All samples were handled on a rigorously pre-conditioned vacuum line fitted with greaseless Young's taps.

### IR laser powered homogeneous pyrolysis

All experimental pyrolysis studies were carried out using the method of infrared laser powered homogeneous pyrolysis, IR LPHP. This technique has been reviewed in detail elsewhere,<sup>35-38</sup> and therefore only a brief description is provided here. Pyrolysis is carried out in a cylindrical Pyrex cell (length 10 cm, diameter 3.8 cm) fitted with ZnSe windows. The cell is filled with a few torr (1 torr = 133.3 Pa) of the vapour under study and approximately 7 torr of SF<sub>6</sub>. The contents of the cell are then exposed to the output of a free running continuous CO<sub>2</sub> laser at a wavelength of 10.6 μm and a power level depending on the temperature required. As shown elsewhere,<sup>35-38</sup> the SF<sub>6</sub> strongly absorbs the laser radiation, which is then converted to heat *via* rapid inter- and intramolecular relaxation. The low thermal conductivity of SF<sub>6</sub> ensures that this process generates a strongly inhomogeneous temperature profile, in which the centre of the cell may reach temperatures as high as 1500 K while the cell walls remain at room temperature.

The IR LPHP technique has a number of well-documented advantages. The first of these is that pyrolysis is initiated directly in the gas phase, eliminating the complications of competing surface reactions frequently encountered in more conventional techniques. The second is that less volatile primary products are rapidly ejected into cool regions of the cell, where they are not subject to further reaction. In favourable cases, these products may be accumulated for further reaction or analysis. Furthermore, the very small quantities of material used render the technique ideal for mechanistic studies involving isotope labelling, and the judicious use of additional reagents in co-pyrolysis studies is straightforward. Finally, we have shown that the technique may be incorporated into a flow system coupled with cryogenic techniques, permitting

the identification of short-lived species through matrix isolation IR or EPR spectroscopy.

On the other hand, the temperature of the pyrolysis is neither well-defined nor easily determined, so that comparison with more conventional methods is not straightforward. Furthermore, the effective temperature is in part determined by the conductivity of the cell contents, and hence may vary over the course of reaction. Despite these factors, an initial effective temperature may be estimated from the rate of disappearance of a compound with known (and comparable) kinetic parameters. In the present experiments, the effective first-order rate constants for thermal decomposition of the target compounds themselves reported by Mackie *et al.*<sup>6,11</sup> and Burcat and Dvinyaninov<sup>17</sup> were used to provide estimates of the pyrolysis temperatures for furan, pyrrole and cyclopentadiene, respectively. It must be emphasised that IR LPHP is a technique with relatively long contact times (several minutes) and product conversions at the same temperature are therefore much higher than those achieved with methods such as shock tube or flash vacuum techniques. Consequently, it is possible to probe considerably lower effective temperatures, with the result that the technique discriminates more strongly in favour of lower activation energy routes when multiple parallel pathways exist.

### Analysis

All stable products were identified by a combination of FTIR and GC/MS. All FTIR spectra were recorded directly (either as vapour or as liquid or solid deposits on the cell windows) using the 10 cm long pyrolysis cell described above. Although the ZnSe windows have a relatively high cut-off at the low frequency end (approximately  $500\text{ cm}^{-1}$ ), for our LPHP work it possesses many advantages over materials such as NaCl or KCl.

All GC/MS work was carried out using a Hewlett Packard 6890 Series II gas chromatograph coupled with a Hewlett Packard 5873 mass selective detector. The GC employed a HPI phenyl methyl siloxane gum capillary column of  $0.33\text{ }\mu\text{m}$  film thickness and  $25\text{ m}$  by  $0.2\text{ mm}$  internal diameter. Pyrolysis samples for GC/MS analysis were taken directly from the pyrolysis cell by means of a rubber septum and a sealable gas-tight syringe. This method possesses several practical advantages over the solvent-based methods used earlier and also is more reliably quantitative.

EPR spectroscopy was carried out using a Varian E-4 EPR spectrometer. Samples for EPR spectroscopy were collected using the methods described in detail elsewhere.<sup>28–30</sup> Briefly, the laser pyrolysis cell is connected to a vacuum line and liquid nitrogen cooled cold finger assembly. A bulb containing the required mixture of  $\text{SF}_6$  and starting material is also attached to the cell and the pyrolysis gas is slowly flowed through the cell while being exposed to the  $\text{CO}_2$  laser radiation. The resulting gas containing pyrolysis products, including any free radical intermediates, is then trapped onto the cold finger. This results in a matrix containing  $\text{SF}_6$ , unreacted starting material and intermediates and final products. The entire cold finger assembly can be demounted and installed into the EPR spectrometer for examination.

For the present study, the technique was modified to incorporate a pressure reduction glass diaphragm between the pyrolysis cell and the cold finger assembly. This permitted pyrolysis at higher pressures than previously, in turn allowing the attainment of significantly higher temperatures and exploration of a wider range of intermediates. Loss of radicals through the diaphragm did not appear to be marked and, in any event, was reduced by coating with  $\text{B}_2\text{O}_3$  to minimise surface-catalysed recombination. The observation (or otherwise) of signals arising from a given free radical depends on its

steady state concentration and hence on its rates of both formation and subsequent decomposition.

### Calculations

When available, relevant results of high level *ab initio* calculations were obtained from the literature. When not available, indicative calculations of structures, energies and transition states were carried out at the *ab initio* (Hartree–Fock 3-21G or 6-31G\*) or B3LYP density functional level using the PC Spartan '02 molecular modelling package.<sup>39</sup> All structures were located by minimising the norm of the analytical energy gradient to less than  $5 \times 10^{-9}$  N. Transition states were located by ensuring that the Hessian matrix (matrix of energy second derivatives) possessed only one negative frequency, corresponding to the reaction coordinate. Reaction coordinates were verified using the visualisation facilities of the package. Although the absolute accuracy of these methods is less than more sophisticated methods reported in the literature, benchmarking against high-level calculations on similar systems has shown that they do provide sufficiently reliable discrimination among possible reaction pathways.

## Results and discussion

### Furan and bromofurans

Of the published studies of the kinetics of the thermal decomposition of furan, two were carried out under the single pulse shock tube conditions that are of most relevance to the present work. Lifshitz *et al.* studied the decomposition of furan at temperatures between 1050 and 1460 K, and concluded that two parallel major routes operate, one leading to the formation of CO and propyne and/or allene, and the second to acetylene and ketene, although ketene was not directly detected in that work.<sup>5</sup> The work of Organ and Mackie<sup>6</sup> covered the temperature range 1100 to 1700 K; in addition to propyne, allene was also identified as a major product. The latter workers concluded that both routes originate in a common first step, that of homolytic C–O bond cleavage resulting in a biradical species. Very recently, Sendt *et al.* have carried out high level *ab initio* calculations on the furan system and concluded that neither C–O nor C–H fission is likely to be a major initiation process; instead, 1,2-H transfers resulting in cyclic carbenes provide the first step in the lowest energy pathways to the observed products.<sup>19</sup>

In the LPHP work reported here, laser powers were set to produce lower temperatures between 950 and 1000 K, as estimated from the rate of disappearance of furan and the effective kinetic parameters of Organ and Mackie.<sup>6</sup> The major products were those reported by earlier workers, with the  $\text{CO} + \text{C}_3\text{H}_4$  route dominating over ketene and acetylene; there was a significant production of benzene in addition (approximately 15%). However, in LPHP the major  $\text{C}_3$  product identified by both FTIR and GC/MS is clearly allene, with very little detectable propyne. Co-pyrolysis with  $\text{H}_2$  (furan: $\text{H}_2 = 1:1$ ) resulted in a modest decrease in allene, propyne and benzene relative to CO, acetylene and ketene; no deuterium incorporation into the initial furan was detected on co-pyrolysis with  $\text{D}_2$ . No EPR signals were observed under any conditions and no furan oligomers were detected.

As shown in our studies of azines, the pyrolysis of brominated analogues can provide additional insight into the significance of radical routes that may operate for the parent compound. Accordingly, the pyrolysis of both 2-bromofuran and 3-bromofuran was studied at temperatures near 850 K in order to identify the part played by furyl radicals. These two compounds yielded almost identical results, but dramatically different from the parent furan. CO and benzene (> 70%) now appear as substantially the major products, with

appreciable quantities of bromobenzene (> 20%) and much smaller amounts of the C<sub>6</sub>H<sub>6</sub> isomers hexa-1,3-dien-5-yne and hexa-1,5-dien-3-yne, acetylene, 1,3-butadiyne, 1-buten-3-yne, and allene or propyne. Again, GC/MS revealed no trace of furan oligomers. Co-pyrolysis with H<sub>2</sub> reduced the yield of C<sub>6</sub>H<sub>6</sub> isomers at the expense of allene and propyne. Relevant regions of the FTIR spectrum of the pyrolysis products of furan and 3-bromofuran are illustrated in Fig. 1.

The very marked change in product distribution on using bromofurans as starting materials and the absence of EPR signals from furan, together with the lack of sensitivity towards co-pyrolysis with H<sub>2</sub>, combine to rule out a significant radical route initiated by C–H bond homolysis in furan. However, the substantial production of benzene from bromofurans (> 70%) confirms the furyl radical as the principal source of benzene, as assumed in earlier work. This conclusion is consistent with the high energy of the C–H bond (over 500 kJ mol<sup>-1</sup> according to the CASPT2 calculations of Sendt *et al.*<sup>19</sup>) compared with less than 300 kJ mol<sup>-1</sup> for 1,2-H shifts.<sup>19</sup> Similar remarks apply to the biradical route arising from C=O homolysis (calculated at slightly below or above 400 kJ mol<sup>-1</sup>, depending on spin state<sup>19</sup>). However, it is clear from the bromofuran results that both 2-furyl and 3-furyl radicals suffer ready loss of CO to yield C<sub>3</sub>H<sub>3</sub>, which is a well-known precursor to benzene.<sup>40</sup> In view of the low energy barrier to H migration in the parent compound, it is likely that the two furyl radicals also interconvert very readily, resulting in identical end products from either precursor. In the presence of H<sub>2</sub>, the C<sub>3</sub>H<sub>3</sub> radicals are evidently trapped as the isomers of C<sub>3</sub>H<sub>4</sub> rather than combining to yield benzene.

Not predicted from earlier work, or by the calculations of Sendt *et al.*,<sup>19</sup> was the almost exclusive production of the allene isomer of C<sub>3</sub>H<sub>4</sub>. These calculations suggest that the first stable intermediate of the ring-opening of the 3,2-hydrogen shifted

cyclic carbene is formyl allene, which subsequently undergoes a 1,4-hydrogen shift and simultaneous C–C σ-bond cleavage to yield CO and propyne. However, it is well-known that formyl allene undergoes ready conversion to the more stable vinyl ketene;<sup>41,42</sup> ketenes very readily decarbonylate and the resultant vinyl methylene is likely to suffer the usual 1,2-hydrogen shift to yield the observed allene. The calculated activation energies of potential reaction pathways are summarised in Table 1 and the dominant reaction pathways for both furan itself and the bromofurans are illustrated in Scheme 1.

### Pyrrole

Two single pulse shock tube studies of pyrrole pyrolysis, by Lifshitz *et al.*<sup>10</sup> and Mackie *et al.*,<sup>11</sup> have covered the temperature ranges 1050–1450 K and 1200–1700 K, respectively. The latter workers identified a reversible 1,2-hydrogen shift to form the unstable pyrrolenine as the first step, followed by C2–N homolysis. The resultant biradical then breaks down in a manner analogous to that for furan, yielding HCN and C<sub>3</sub>H<sub>4</sub> (allene or propyne) or acetylene and acetonitrile. Alternatively, it may rearrange to form the CN-terminal pyrrole isomers allyl cyanide or crotonitrile in a route not available for furan. As in the case of furan, there have been several recent high-level calculations in an attempt to discriminate among possible initiation routes.<sup>20–23</sup> All these theoretical studies have confirmed the relatively high N–H bond energies in pyrrole (397 kJ mol<sup>-1</sup> at the CASPT2 level<sup>20</sup>) and our own calculations show that direct C–H fission at either the 2 or 3 positions is even less favourable at 473 and 444 kJ mol<sup>-1</sup>, respectively. Direct ring C–N or C–C scissions are also unfavourable, at 393 and 557 kJ mol<sup>-1</sup>, respectively.<sup>23</sup> As in the case of furan, the most likely routes involve 1,2-hydrogen shifts, yielding initially cyclic

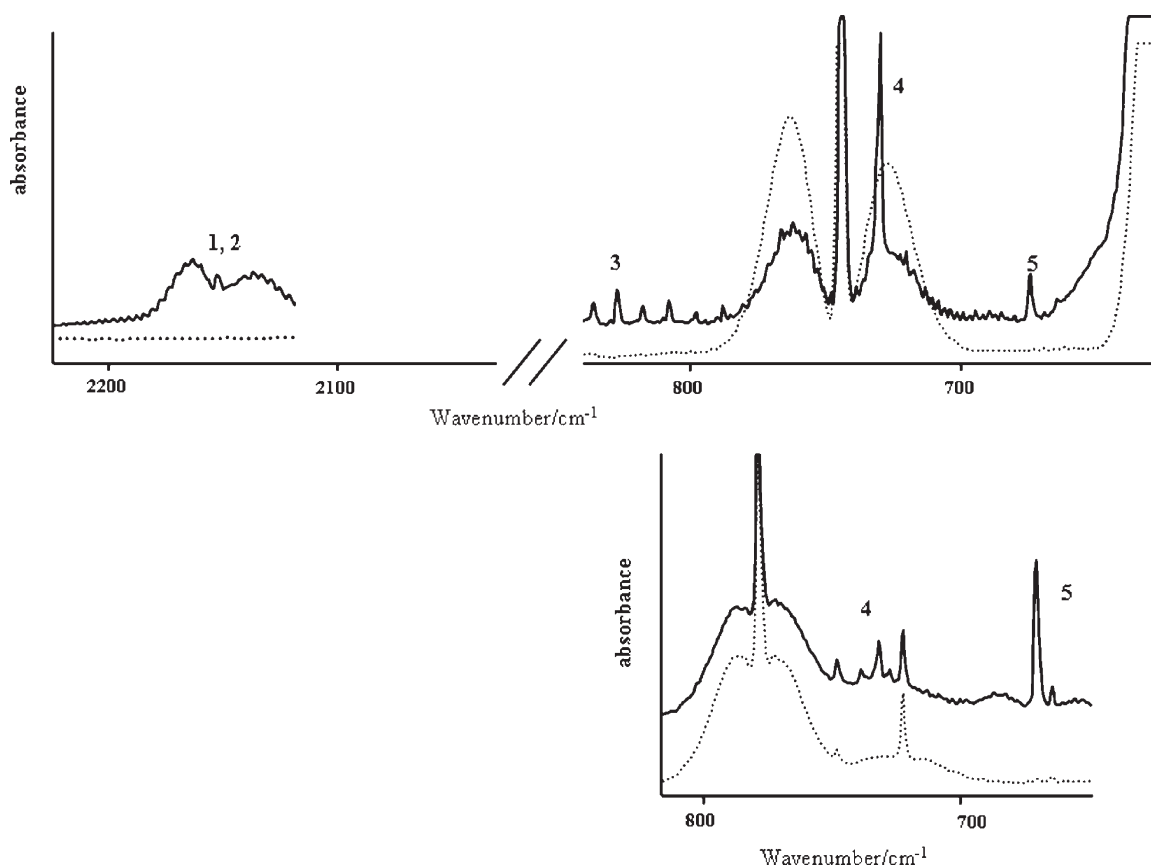


**Fig. 1** Partial FTIR spectra of the products of IR LPHP of furan (above) and 3-bromofuran (below). Dotted line = before pyrolysis, full line = after pyrolysis. Peaks are labelled as: 1 = ketene, 2 = CO, 3 = allene, 4 = acetylene, 5 = benzene; unassigned peaks are due to starting material or SF<sub>6</sub>.

**Table 1** Structures and calculated energies of possible initial intermediates in the thermal decomposition of 5-membered rings<sup>a</sup>

Number	I	II	III	VI	V	VI	VII
Structure							
A = CH <sub>2</sub>	0	–	–	346/346/379 <sup>b</sup>	310/309/428 <sup>b</sup>	306/275/393 <sup>b</sup>	167/0 <sup>g</sup>
A = NH	0	494/494 <sup>f</sup>	492/492 <sup>f</sup>	Polyaromatics 397/397 <sup>e</sup>	C <sub>2</sub> H <sub>2</sub> + allene 258/203 <sup>d</sup>	C <sub>2</sub> H <sub>2</sub> + propyne 302/265/332 <sup>d</sup>	– 190/58/317 <sup>d</sup>
A = O	0	495/495 <sup>f</sup>	495/495 <sup>f</sup>	–	270/229/346 <sup>e</sup>	HCN + propyne 290/245/275 <sup>e</sup>	– Cyanopropenes
A = S	0	488/488/488 <sup>f</sup> Bisthiophene	476/476/476 <sup>f</sup> Bisthiophene	–	C <sub>2</sub> H <sub>2</sub> + H <sub>2</sub> CCO 305/261/590 <sup>g</sup>	CO + C <sub>3</sub> H <sub>4</sub> 326/279/611 <sup>g</sup>	–

<sup>a</sup> All energies in kJ mol<sup>-1</sup>. A = CH<sub>2</sub>, NH, O or S; A' = CH or N. For each numerical entry, the first number is the energy of the transition state for formation, the second the energy of the species, and the third (where given) the energy of the transition state for subsequent decomposition, all relative to the parent compound; the major products of the specified decomposition route are also listed for each species. <sup>b</sup> Ref 24. <sup>c</sup> Ref 20. <sup>d</sup> Ref 23. <sup>e</sup> Ref 19. <sup>f</sup> Ref 46. <sup>g</sup> This work (B3LYP).

carbenes (or, in the case of pyrrole, pyrrolenine), followed by ring opening and rearrangement.

IR LPHP of pyrrole at temperatures between 1000 and 1050 K confirmed *cis*- and *trans*-crotonitrile (*E*- and *Z*-1-cyanopropene, 20% and 9%, respectively) and allyl cyanide (3-cyanopropene, 11%) as the major low temperature pyrolysis products. In addition, significant amounts of acrylonitrile (cyanoethene, 16%), acetylene, HCN and allene or propyne (38%) were also produced, together with benzene and other C<sub>6</sub>H<sub>6</sub> isomers in smaller quantities (5% total). A typical GC-MS trace is shown in Fig. 2. Only very weak EPR signals were detectable, indicating a very minor radical route; no pyrrole oligomers were detected.

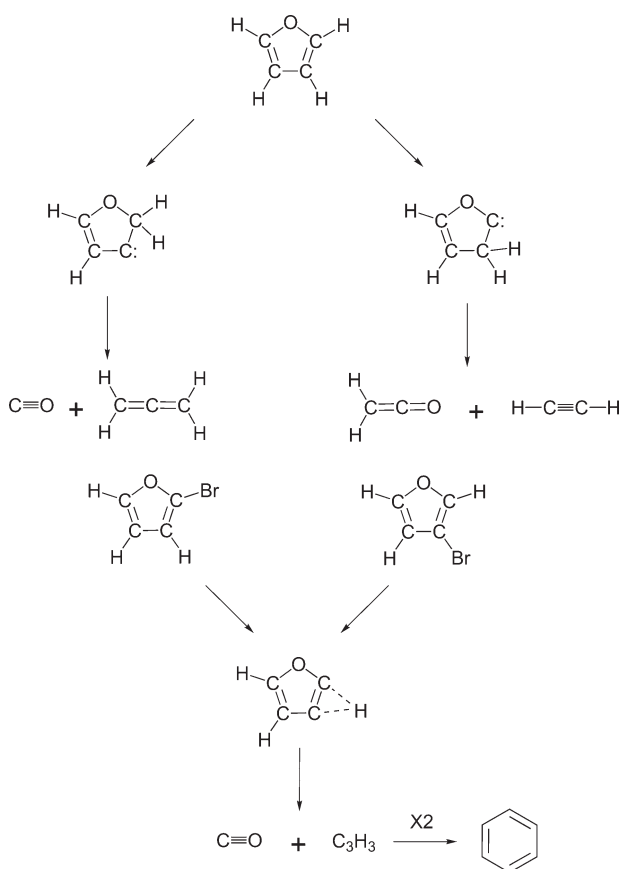
Co-pyrolysis with H<sub>2</sub> suppressed the formation of benzene and on co-pyrolysis with D<sub>2</sub>, some deuteration of the open-chain pyrrole isomers was detected, but none of the residual pyrrole. Unfortunately, C-substituted bromopyrroles are well-known to be unstable towards auto-polymerisation,<sup>43–45</sup> precluding any study of these compounds; other potential sources of pyrrolyl radicals do not lend themselves readily to comparison with the IR LPHP observations.

The IR LPHP results are entirely consistent with earlier investigations and the results of high-level calculations and so little additional insight into the decomposition mechanism for this compound is afforded. The calculated activation energies of potential reaction pathways are summarised in Table 1 and the dominant reaction pathways for pyrrole are illustrated in Scheme 2.

### Cyclopentadiene

There have been several experimental studies of the thermal decomposition of cyclopentadiene.<sup>12–17</sup> The major products at high temperatures are polycyclic aromatics such as naphthalene, *etc.*; at lower temperatures, products include relatively minor quantities of benzene, acetylene and allene and/or propene. It has generally been accepted that the principal initiation step in the pyrolysis of cyclopentadiene is H loss to form the stable *c*-C<sub>5</sub>H<sub>5</sub> radical; however, to our knowledge, there has been no prior report of the direct confirmation of this process. Following their similar studies of the isoelectronic furan and pyrrole, Bacskay and Mackie have carried out *ab initio* calculations at the CASPT2 level and have shown that 1,2-H shifts to produce cyclic carbenes may also be very important in the production of C<sub>2</sub>H<sub>2</sub> and C<sub>3</sub>H<sub>4</sub> in the cyclopentadiene case.<sup>24</sup>

IR LPHP of cyclopentadiene led to an extensive array of products; the major products detectable by GC/MS included benzene (51%) and the other aromatic hydrocarbons identified by previous workers, predominantly toluene (20%), naphthalene (12%), styrene (7%) and indene (4%). Higher molecular weight products may also be formed, but are unlikely to have sufficient vapour pressure to be recovered for GC/MS analysis. Low molecular weight products in relatively low yield included methane, acetylene, propyne and/or allene, 1,3-butadiene and but-1-ene-3-yne. Co-pyrolysis with excess H<sub>2</sub> led to a reduction in the aromatic products at the expense of smaller products, while co-pyrolysis with D<sub>2</sub> led to extensive deuteration of residual cyclopentadiene. Significantly, the benzene product was not deuterated at all, while the allene was



**Scheme 1** Major pathways in the thermal decomposition of furan (above) and the bromofurans (below); activation energies are given in Table 1.

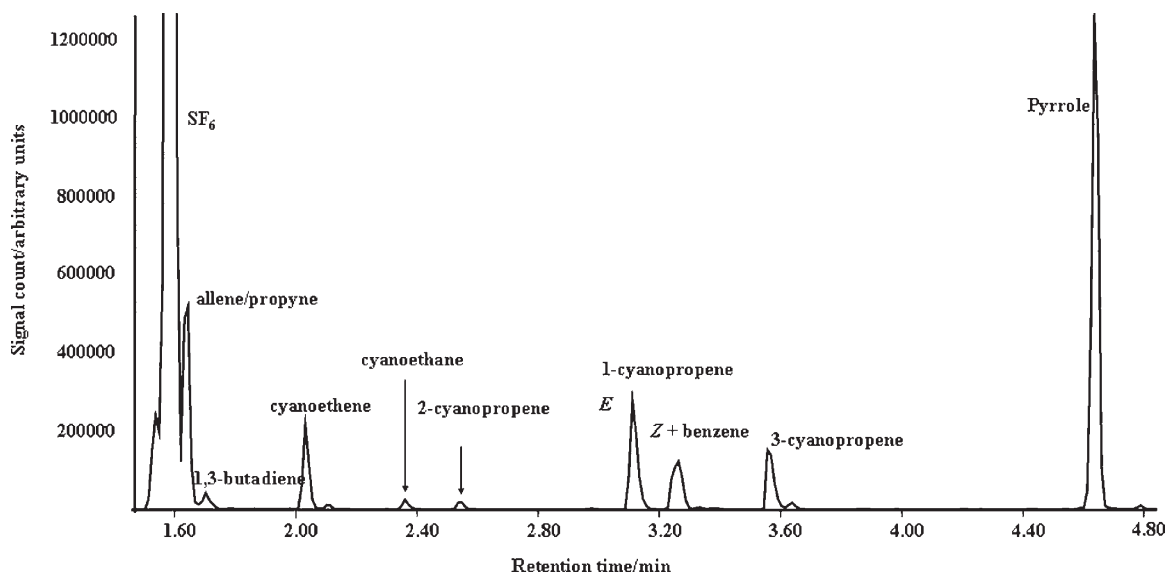
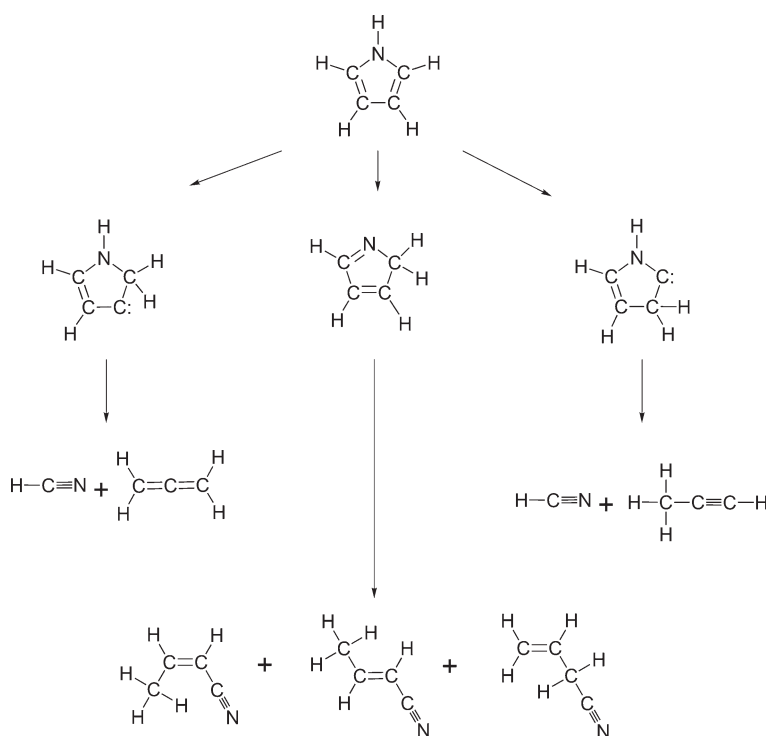


Fig. 2 Gas chromatogram of products of IR LPHP of pyrrole.

very heavily deuterated (the ratio of mass 41 to mass 40 was almost 3:1 in the presence of  $D_2$ , while this ratio was 1:20 in the absence of  $D_2$ ). Very strong EPR signals, unambiguously attributable to cyclopentadienyl radicals, were observed, as shown in Fig. 3. Brominated compounds were considered unlikely to reveal additional information in this case and no study of these was undertaken.

Clearly,  $C_5H_5$  radicals are formed in very substantial quantities, but are relatively stable to the further breakdown to  $C_2H_2$  and  $C_3H_3$  assumed in some earlier work.<sup>12–17</sup> Instead, they recombine with loss of  $H_2$  to form largely naphthalene, as shown in our work on cyclopentadienyl containing transition metal compounds and elsewhere,<sup>28</sup> while well-attested, the detailed mechanism of this step is unknown and merits further theoretical investigation. The extensive D-incorporation observed on co-pyrolysis with  $D_2$  implies considerable

back reaction, almost certainly involving H atoms, since the reaction of  $C_5H_5$  with  $H_2$  is endothermic to the extent of some  $100 \text{ kJ mol}^{-1}$ . It is therefore reasonable to conclude that these radicals do not break down, but recombine in a number of ways to yield the observed polyaromatic hydrocarbons (and eventually soot, at higher temperatures still). This conclusion is in agreement with the calculations of Bacskay and Mackie,<sup>24</sup> as well as those of other theoretical investigations;<sup>46</sup> thus the C–H bond strength is calculated to be  $343 \text{ kJ mol}^{-1}$  at the CASPT2 level, while the subsequent steps of 1,2-H shift and C–C bond fission require a further  $403 \text{ kJ mol}^{-1}$ . Bacskay and Mackie have further asserted that the small molecule route is therefore unlikely to involve  $C_5H_5$  radicals and instead follows 1,2-H shifts to yield cyclic carbenes, followed by ring opening and C–C fission; the activation energies of the two possible routes were found to be 393 and  $427 \text{ kJ mol}^{-1}$ . There



Scheme 2 Major pathways in the thermal decomposition of pyrrole; activation energies are given in Table 1.

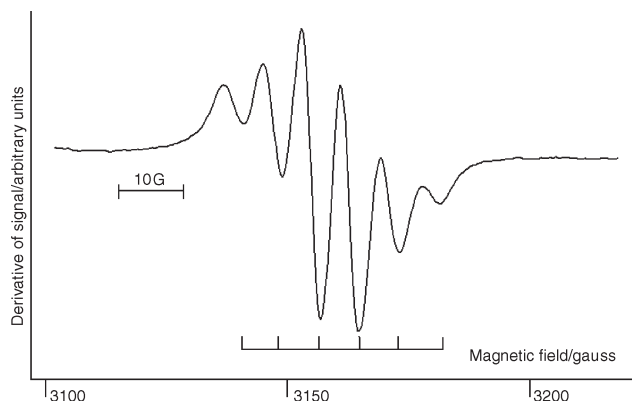
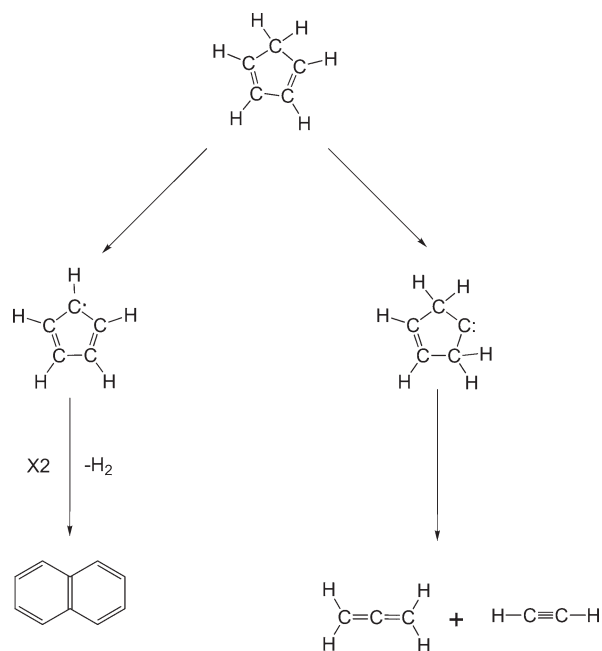


**Fig. 3** EPR spectrum of free radicals produced in the IR LPHP of cyclopentadiene.

is some support for this assertion in the analogous saturated cyclopentylidene carbene. When formed through low energy routes [such as abstraction of the O atom from cyclopentanone by  $W(CO)_n$  in IR LPHP<sup>47</sup>] only the 1,2-H migration product cyclopentene is observed, whereas the high energy carbene (formed by O-abstraction by C atoms) also leads to appreciable quantities of allene and ethylene.<sup>48</sup> The calculated activation energies of potential reaction pathways are summarised in Table 1 and the dominant reaction pathways for cyclopentadiene are illustrated in Scheme 3.

### Thiophene and bromothiophenes

There have been very few detailed studies of the thermal decomposition of thiophene, apart from a brief report on the production of bithiophenes in a study of the relative thermal stability of a series of heterocycles by Bruinsma *et al.*<sup>1</sup> A recent analysis of breakdown products has confirmed bithiophenes as the major product at temperatures below 1100 K, with significant production of  $CS_2$  and sulfur-containing polyaromatics as the temperature is raised.<sup>18</sup> The reason for this is the thermal stability of the compound; it is frequently encountered as an end product of the thermolysis of sulfur-containing



**Scheme 3** Major pathways in the thermal decomposition of cyclopentadiene; activation energies are given in Table 1.

organic systems and is a major sulfur-containing component of fossil fuels.

IR LPHP of thiophene at laser powers estimated to produce temperatures of 1150 to 1200 K resulted in solid deposits of polythiophene, with acetylene as the major gas phase product; trace quantities of benzene and methane were observed after prolonged laser exposure. In addition, considerable quantities of the three isomeric bithiophenes were observed, constituting over 60% of the observable products, as well as smaller quantities of benzothiophene and phenylthiophene. At higher laser powers,  $CS_2$  and increased amounts of polyaromatics were also observed. Co-pyrolysis of thiophene with  $D_2$  (thiophene: $D_2$  = 1:1) produced the FTIR spectrum of Fig. 4. This shows very clear evidence of extensive deuteration of the parent at both the 2 and 3 positions, together with peaks attributable to more highly deuterated products; this is confirmed by GC-MS. Very weak EPR signals were observed, but could not be analysed satisfactorily. LPHP of 2-Br and 3-Br thiophene (at much lower laser powers) resulted in the production of methane and thiophene itself, as well as deposits identified as polythiophene. All three isomeric bithiophenes were again observed, with product ratios dependent to some extent on the nature of the starting material. Co-pyrolysis of the bromo compounds with  $D_2$  also resulted in extensively deuterated thiophene. The relative yields of the isomeric bithiophenes are illustrated in Fig. 5.

The higher temperature required to decompose thiophene is consistent with the absence of a low activation energy initiation step. Calculations place C–H bond strengths at  $490 \text{ kJ mol}^{-1}$ <sup>49</sup> and the ring C–S bond at  $560 \text{ kJ mol}^{-1}$ . By analogy with its lighter analogues, 1,2-H transfer is the most probable step (activation energy  $300 \text{ kJ mol}^{-1}$ ), but it is clear from the results above that both thienyl radicals and any ring carbenes must also be sufficiently stable to internal reaction to allow for extensive exchange reactions before bond fission. It is entirely reasonable to assume that recombination of thienyl radicals leads to the major observed products, the isomeric bithiophenes, although radical reaction with the parent cannot be ruled out. The calculated activation energies of potential reaction pathways are summarised in Table 1 and the dominant reaction pathways for both thiophene itself and the bromothiophenes are illustrated in Scheme 4.

### Conclusions

Decomposition of the compounds described here may conceivably be initiated by one or more of a number of steps, which are discussed in turn below.

(i) *Direct* scission of a ring C–C or heteroatom–C bond will result in biradicals or linear carbenes. However, all calculations have shown that this route demands very high energy; direct C–O bond scission to produce the lowest triplet state of a linear carbene from furan requires  $322 \text{ kJ mol}^{-1}$  (at the CASPT2 level<sup>19</sup>) and other molecules require even higher energies (for thiophene, for example,  $560 \text{ kJ mol}^{-1}$  at the Hartree–Fock level). It should be noted that further energy barriers to decomposition of these initial intermediates are also substantial. We therefore conclude that direct ring-bond scission is unlikely to be the lowest energy initiation step in any system, and it will not be considered further.

(ii) Scission of a ring C–H or heteroatom–H bond will produce cyclic free radicals. C–H bond strengths for a range of pyrrolic compounds and the N–H strength in pyrrole have recently been calculated at the B3LYP/6-31G level.<sup>49</sup> C–H scission generally requires on the order of  $500 \text{ kJ mol}^{-1}$ , the notable exception being cyclopentadiene at  $346 \text{ kJ mol}^{-1}$ . This step is likely to be important only when lower energy routes are unavailable, as in cyclopentadiene and thiophene. Since C–Br scission in the brominated compounds is undoubtedly

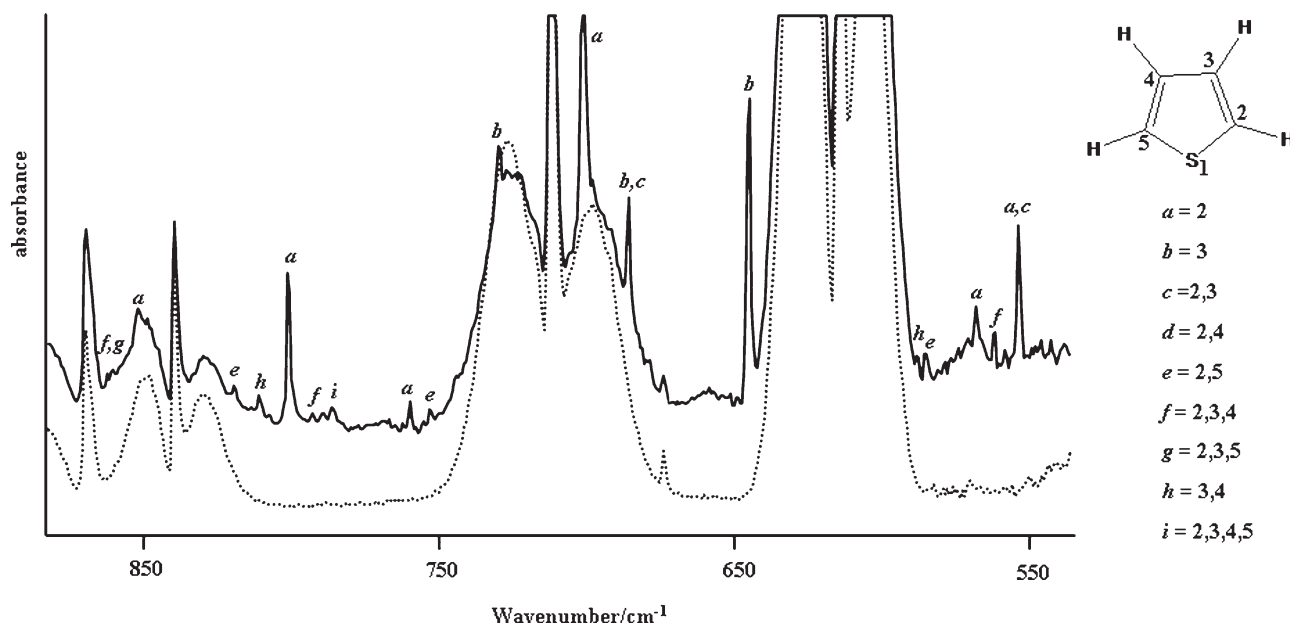


**Fig. 4** Partial FTIR spectrum of the products of IR LPHP of a 1:1 mixture of thiophene and  $D_2$ . Dotted line = before pyrolysis, full line = after pyrolysis. Labelled peaks are assigned to partially deuterated thiophene as indicated; unassigned peaks are due to starting material or  $SF_6$ .

the lowest energy step, the products of radical pathways in these compounds provide a clear indication of the ultimate fate of such radicals.

(iii) *Indirect* ring-bond scission, preceded by 1,2-H shifts from C to C or C to heteroatom (or *vice versa*), results in carbenes, followed by ring opening and rearrangement. This appears to be the lowest energy route in furan and pyrrole, and may also contribute to small molecule production in cyclopentadiene—it appears to be insignificant in the study of thiophene in the present work, however.

The calculated relative energies of the relevant steps for pathways (ii) and (iii) are given in Table 1, which will serve as a basis for drawing general conclusions.

The pivotal role of cyclopentadienyl radicals is graphically confirmed by their direct observation by EPR and supported by isotope exchange on co-pyrolysis of cyclopentadiene in the presence of  $D_2$ . Similarly, the observation of bisthiophenes as the major product of thiophene supports the role of C-centred radicals in this system, a view supported by the

observation of identical products using bromothiophenes as radical sources. On the other hand, the lower ring bond dissociation energy in cyclopentadienyl also leads to the observation of small molecule products, in contrast with thiophene. The relative unimportance of radical routes in furan and pyrrole is also confirmed by our observations; this is confirmed by the observation of very different products using bromofurans as a source of furyl radicals. In these latter systems, the initial steps are 1,2-hydrogen shifts, followed by internal scission and/or rearrangement of the cyclic carbenes. These assertions are confirmed by the calculations reported in Table 1, which in each case indicate that the lowest energy predicted pathway leads to the observed products.

The role played by the cyclic carbenes formed by 1,2-H shifts in cyclopentadiene, furan and pyrrole, strongly indicated by relative activation energy calculations, will be explored in future work by direct generation using the method of O-abstraction from suitable carbonyl precursors by  $W(CO)_n$  species recently discovered in our laboratory.<sup>48</sup>

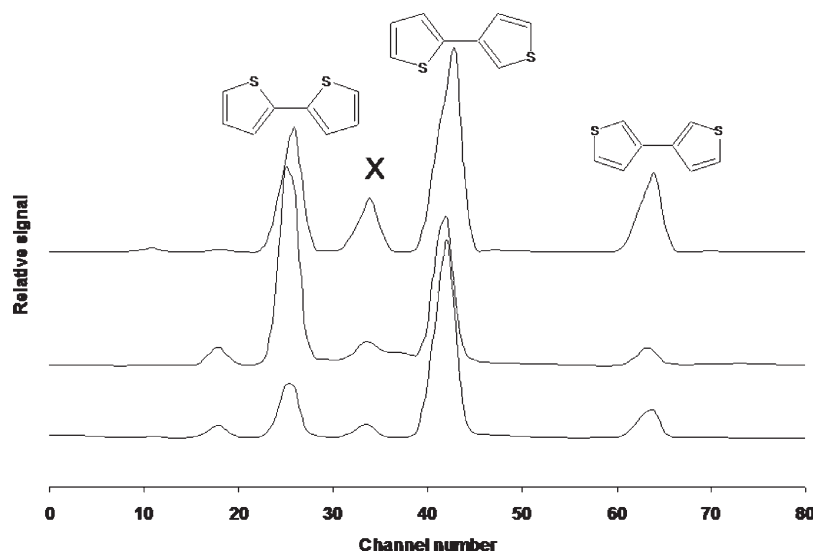
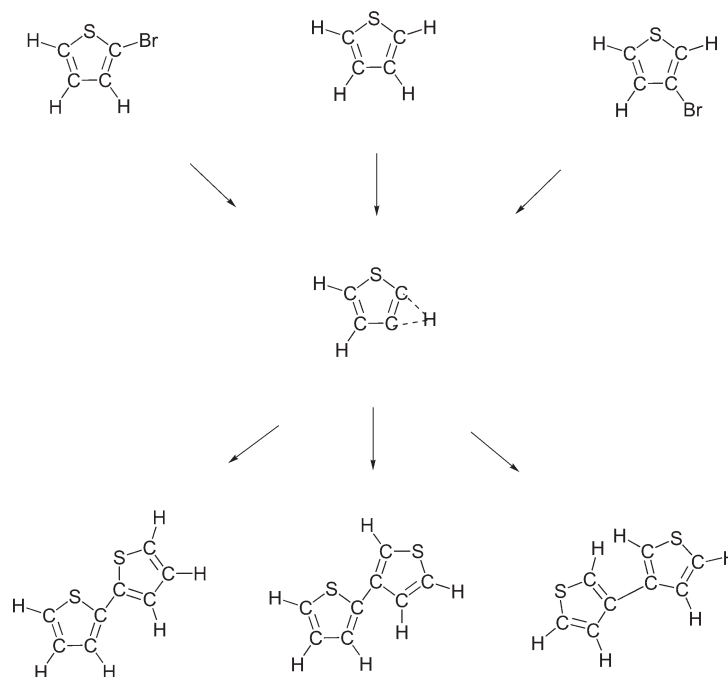


**Fig. 5** Partial gas chromatogram of the products of IR LPHP of thiophene (top trace), 2-bromothiophene (middle trace) and 3-bromothiophene (bottom trace), indicating relative yields of 2,2-bisthiophene, 2,3-bisthiophene and 3,3-bisthiophene. The peak marked X arises from one isomer of phenylthiophene, the second isomer being obscured.



**Scheme 4** Major pathways in the thermal decomposition of thiophene and the bromothiophenes; activation energies are given in Table 1.

## Acknowledgements

The authors gratefully acknowledge financial support from the Department of Chemistry and the Research Committee of the University of Auckland, and useful correspondence with Professor J. C. Mackie of the University of Sydney.

## References

- D. S. C. Bruinsma, P. J. J. Tramp, H. J. J. de Sauvage Nolting and J. A. Moulijn, *Fuel*, 1988, **67**, 334.
- G. Holzner, J. Oro and W. Bertsch, *J. Chromatogr.*, 1976, **126**, 771.
- G. Schopf and G. Kobmehl, *Polythiophenes-Electrically Conductive Polymers*, Springer, Berlin, 1997 and references therein.
- M. A. Grela, V. T. Amorebieta and A. J. Colussi, *J. Phys. Chem.*, 1985, **89**, 38.
- A. Lifshitz, M. Bidani and S. Bidani, *J. Phys. Chem.*, 1986, **90**, 5373.
- P. P. Organ and J. C. Mackie, *J. Chem. Soc., Faraday Trans.*, 1991, **87**, 815.
- J. M. Patterson, A. Tsamasfyros and W. T. Smith, *J. Heterocycl. Chem.*, 1968, **5**, 727.
- W. R. Johnson and J. C. Kang, *J. Org. Chem.*, 1971, **36**, 189.
- A. E. Axworthy, V. H. Dayan and G. B. Martin, *Fuel*, 1978, **57**, 29.
- A. Lifshitz, C. Tamburu and A. Suslensky, *J. Phys. Chem.*, 1989, **93**, 5802.
- J. C. Mackie, M. B. Colkett, P. F. Nelson and M. Esler, *Int. J. Chem. Kinet.*, 1991, **23**, 733.
- M. Szwarc, *Chem. Rev.*, 1950, **47**, 135.
- R. Spielman and C. A. Cramers, *Chromatographia*, 1972, **5**, 295.
- E. Gey, B. Ondrushka and G. Zimmerman, *J. Prakt. Chem.*, 1987, **329**, 511.
- R. G. Butler, *MSc Thesis*, Princeton University, Princeton, NJ, USA, 1992.
- M. B. Colket, *The Pyrolysis of Cyclopentadiene*, Eastern States section of the Combustion Institute Annual Meeting in Orlando, FL, 1990.
- A. Burcat and M. Dvinyaninov, *Int. J. Chem. Kinet.*, 1997, **29**, 505.
- J. K. Winkler, W. Karow and P. Rademacher, *J. Anal. Appl. Pyrolysis*, 2002, **62**, 123.
- K. Sendt, G. B. Bacskay and J. C. Mackie, *J. Phys. Chem. A*, 2000, **104**, 1861.
- G. B. Bacskay, M. Martoprawiro and J. C. Mackie, *Chem Phys. Lett.*, 1998, **290**, 391.
- G. B. Bacskay, M. Martoprawiro and J. C. Mackie, *Chem Phys. Lett.*, 1999, **300**, 321.
- L. Zhai, X. Zhou and R. Liu, *J. Phys. Chem. A*, 1999, **103**, 3917.
- M. Martoprawiro, G. B. Bacskay and J. C. Mackie, *J. Phys. Chem. A*, 1999, **103**, 3923.
- G. B. Bacskay and J. C. Mackie, *Phys. Chem. Chem. Phys.*, 2001, **3**, 2467.
- N. R. Hore and D. K. Russell, *J. Chem. Soc., Perkin Trans. 2*, 1998, 269.
- D. K. Russell, *Coord. Chem. Rev.*, 1992, **112**, 131.
- A. S. Grady, R. D. Markwell and D. K. Russell, *J. Chem. Soc., Chem. Commun.*, 1991, 929.
- D. K. Russell, I. M. T. Davidson, A. M. Ellis, G. P. Mills, M. Pennington, I. M. Povey, J. B. Raynor, S. Saydam and A. D. Workman, *Organometallics*, 1995, **14**, 3717.
- D. K. Russell, G. P. Mills, J. B. Raynor and A. D. Workman, *Chem. Vap. Deposition*, 1998, **4**, 61.
- D. K. Russell, I. M. T. Davidson, A. M. Ellis, G. P. Mills, M. Pennington, I. M. Povey, J. B. Raynor and S. Saydam, *Chem. Vap. Deposition*, 1998, **4**, 103.
- R. A. Berrigan, J. B. Metson and D. K. Russell, *Chem. Vap. Deposition*, 1998, **4**, 23.
- J. E. Everett, N. D. Renner and D. K. Russell, *Chem. Commun.*, 1998, 341.
- G. R. Allen, N. D. Renner and D. K. Russell, *Chem. Commun.*, 1998, 703.
- E. L. Clennan and M. E. Mehrsheikh-Mohammabi, *J. Am. Chem. Soc.*, 1984, **106**, 7112.
- W. M. Shaub and S. H. Bauer, *Int. J. Chem. Kinet.*, 1975, **7**, 509.
- J. Pola, *Collect. Czech. Chem. Commun.*, 1981, **46**, 2856.
- D. K. Russell, *Chem. Soc. Rev.*, 1990, **19**, 407.
- D. K. Russell, *Chem. Vap. Deposition*, 1996, **2**, 223 and references therein.
- Spartan '02*, Wavefunction Inc., Irvine, CA, USA, 2002.
- J. A. Miller, R. J. Kee and C. K. Westbrook, *Ann. Rev. Phys. Chem.*, 1990, **41**, 345.
- H. Bibas, M. W. Wong and C. Wentrup, *J. Am. Chem. Soc.*, 1995, **117**, 9382.
- H. Bibas, M. W. Wong and C. Wentrup, *Chem.-Eur. J.*, 1997, **3**, 237.
- G. A. Cordell, *J. Org. Chem.*, 1975, **40**, 3161.
- H. M. Gilow and D. E. Burton, *J. Org. Chem.*, 1981, **46**, 2221.
- P. Audebert and G. Bidan, *Synth. Met.*, 1986, **15**, 9.
- L. V. Moskaleva and M. C. Lin, *J. Comput. Chem.*, 2000, **21**, 415.
- G. R. Allen and D. K. Russell, *Chem. Commun.*, 2002, 1960.
- G. Xu, T.-M. Chang, J. Zhou, M. L. McKee and P. B. Shevlin, *J. Am. Chem. Soc.*, 1999, **121**, 7150.
- C. Barckholtz, T. A. Barckholtz and C. M. Hadad, *J. Am. Chem. Soc.*, 1999, **121**, 491.